Creation and Measurement of a Coherent Superposition of Quantum States

Frank Vewinger,* Manfred Heinz, Ruth Garcia Fernandez, Nikolay V. Vitanov,† and Klaas Bergmann‡

Fachbereich Physik der Universität, Erwin-Schrödinger-Strasse, 67653 Kaiserslautern, Germany

(Received 3 June 2003; published 19 November 2003)

We demonstrate experimental techniques for creating and measuring a coherent superposition of two degenerate atomic states with equal amplitudes in metastable neon. Starting from state $^3P_0$, we create adiabatically a coherent superposition of the magnetic sublevels $M = \pm 1$ of the state $^3P_2$ using a tripod stimulated Raman adiabatic passage scheme. The measurement is based on the coupling of the levels $^3P_2 \leftrightarrow {}^3P_1$ by a linearly polarized laser, followed by the detection of the population in the $^3P_2(M = \pm 2)$ states as a function of the polarization angle of that laser.

DOI: 10.1103/PhysRevLett.91.213001 PACS numbers: 32.80.Qk, 03.65.Vf, 03.67.Hk, 42.50.Gy

The creation and measurement of a coherent superposition of quantum states is a crucial ingredient in many applications in quantum physics. The simplest technique that can create superpositions is the π-pulse method which uses resonant pulses of precise area. This technique requires, besides an exact resonance, precise knowledge of the transition moment and control of the amplitude of the external field. Adiabatic evolution provides a solution to this sensitivity because it ensures robustness of the created state against small-to-moderate variations in the interaction parameters, as long as adiabaticity is maintained. Here, we demonstrate experimentally an efficient and robust technique for creating a coherent superposition of two states based on tripod-STIRAP [1,2], which is an extension of the well-known technique of stimulated Raman adiabatic passage (STIRAP) [3]. In comparison to STIRAP, tripod-STIRAP uses an additional, third radiation field, which provides a greater flexibility. Thus, in addition to complete population transfer, tripod-STIRAP can produce coherent superpositions of the three ground states with arbitrary parameters. In a second step, we demonstrate an independent technique for measuring the phase of the created superposition. This scheme is suitable to prove the reliability of the present or other creation techniques. The proposed creation and measurement techniques, for instance, have potential applications in quantum information [4], with a future development of creating entanglement. In experimental implementations of qubits in ion traps [5] and nuclear-magnetic resonance [6] the π-pulse technique is well developed. In other realizations, such as quantum dots [7], Josephson junctions [8], and crystal lattices [9], the coupling strength is often either not known precisely or difficult to measure. In such systems, the π-pulse technique may lead to intolerable inaccuracies and the proposed technique may resolve this difficulty. Quantum systems in superpositional states have also important applications in numerous areas across quantum physics, such as quantum optics [10], cavity QED [11], atom optics [12], electromagnetically induced transparency [13], lasing without inversion [14], control of chemical reactions [15], high harmonic generation [16], and others.

Specifically we report the experimental preparation and measurement of a superposition between the Zeeman sublevels $M = \pm 1$ of the metastable state $^3P_2$ in neon. The superposition is created using tripod-STIRAP, with the coupling scheme shown in Fig. 1. The initially populated state $(2p^5 3s)\ ^3P_0$ is coupled by π-polarized light (referred to as pump laser P) to the intermediate state $(2p^5 3p)\ ^3P_1(M = 0)$, which in turn is coupled to the final states $(2p^5 3s)\ ^3P_2(M = \pm 1)$ by σ^+ and σ^- polarized light, respectively, (referred to as Stokes lasers S_+ and S_-). The two Stokes fields are produced by a linear polarized laser beam (which can be viewed as an equal superposition of σ^+ and σ^- polarizations), and hence they have the same time dependence. The pump field is spatially offset downstream but overlapped with the Stokes fields, as shown in Fig. 2, thus producing a STIRAP-type interaction sequence.

The Hamiltonian of a resonant tripod system [see Fig. 1(a)] has four adiabatic states [1] that are parametrized by two mixing angles $\vartheta(t)$ and $\varphi(t)$, defined

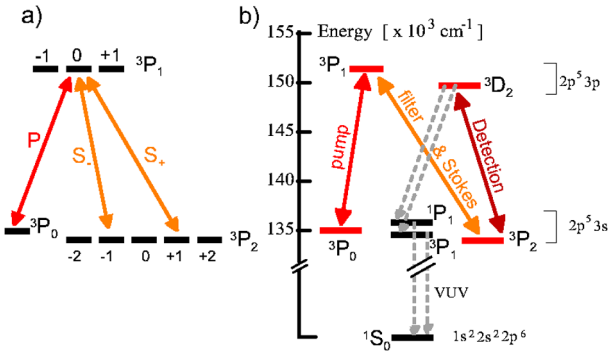

FIG. 1 (color online). (a) Coupling scheme for the creation of the coherent superposition using tripod-STIRAP. (b) Level scheme of ^{20}Ne including the levels involved in the experiment. Dashed lines represent spontaneous emission used in the detection.

 0031-9007/03/91(21)/213001(4)$20.00

by $\tan\vartheta(t) = \Omega_P(t)/\Omega_S(t)$ and $\tan\varphi(t) = \Omega_{S_-}(t)/\Omega_{S_+}(t)$, where Ω_x ($x = P, S_+, S_-$) are the Rabi frequencies of the coupling lasers and $\Omega_S(t) = \sqrt{\Omega_{S_+}^2(t) + \Omega_{S_-}^2(t)}$. Two of the adiabatic states are orthogonal degenerate dark states, i.e., states without components of the intermediate state $^3P_1$,

$$|\Phi_1(t)\rangle = \cos\vartheta(t)|0,0\rangle - \sin\vartheta(t)\cos\varphi(t)e^{-i\chi}|2,-1\rangle - \sin\vartheta(t)\sin\varphi(t)e^{+i\chi}|2,+1\rangle, \quad (1a)$$

$$|\Phi_2(t)\rangle = \sin\varphi(t)e^{-i\chi}|2,-1\rangle - \cos\varphi(t)e^{+i\chi}|2,+1\rangle, \quad (1b)$$

where the states are labeled in the $|J, M\rangle$ notation. The angle χ is defined in Fig. 2. The coupling between these dark states, $\langle\Phi_1(t)|\dot{\Phi}_2(t)\rangle = \dot{\varphi}(t)\sin\vartheta(t)$, induces a (resonant) transition between them, which has been used by Theuer *et al.* [2] to implement a variable atomic beam splitter. In the present experiment, there is only one linearly polarized Stokes laser, which produces two coincident and copropagating σ^+ and σ^- fields with the same intensity; hence $\Omega_{S_-}(t) = \Omega_{S_+}(t)$ and $\varphi \equiv \pi/4$. The implication is that the nonadiabatic coupling between the dark states vanishes identically because $\dot{\varphi} = 0$. Moreover, because the pump field is delayed with respect to the Stokes field, we have $\vartheta(-\infty) = 0$ and $\vartheta(+\infty) = \pi/2$. Hence, in the adiabatic limit, the atom evolves along the adiabatic path $|\Phi_1(t)\rangle$ [1,2] from the initial state $|0,0\rangle$ to the final state $|\Psi\rangle$ with

$$|\Psi\rangle = \frac{1}{\sqrt{2}}[|2,-1\rangle e^{-i(\chi+\phi)} + |2,+1\rangle e^{+i(\chi+\phi)}], \quad (2)$$

where ϕ is an arbitrary phase, e.g., from an external magnetic field.

The measurement of the superposition is based upon mapping the superposition parameters onto the populations of a subset of the M states. This is done by exposing the atoms to a linear polarized "filter" laser, which couples the M' sublevels of the $^3P_2 \leftrightarrow {}^3P_1$ transition

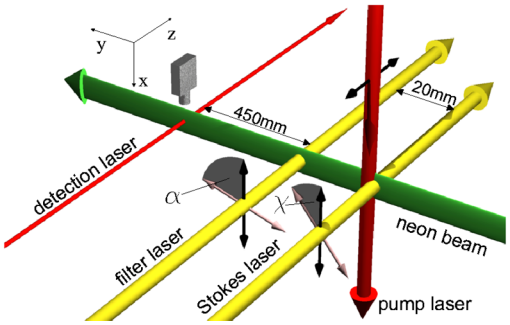

FIG. 2 (color online). Geometry of the experiment. The direction of polarization $\hat{e}_P$ (indicated by the small arrows) for the pump laser P ($\lambda = 616$ nm) is chosen to be the z axis, its direction of propagation defines the x axis, while the neon beam propagates in the y direction. The two circularly polarized Stokes lasers (S_+ and S_-) are generated by a linearly polarized laser ($\lambda = 588$ nm) propagating in the z direction, whose direction of polarization forms an angle χ with the x axis. The propagation of the so-called filter laser ($\lambda = 588$ nm) is parallel to the Stokes laser and its direction of polarization $\hat{e}_F$ forms an angle α with the x axis. The detection laser ($\lambda = 633$ nm) is unpolarized.

with $\Delta M' = 0$, where the quantum number M' is defined with respect to the direction of polarization $\hat{e}_F$ of the filter laser. The resulting state vector $|\Psi'\rangle$ in this frame of reference (defined by $\hat{z}' \parallel \hat{e}_F$) is

$$|\Psi'\rangle = \hat{R}(\alpha,\beta,\gamma)|\Psi\rangle = e^{-i\gamma\hat{J}_z}e^{-i\beta\hat{J}_y}e^{-i\alpha\hat{J}_z}|\Psi\rangle, \quad (3)$$

where $\hat{R}$ is the rotation operator and α, β, and γ are the Euler angles [17]. For the choice of $\beta = \pi/2$ (corresponding to $\hat{e}_P \perp \hat{e}_F$) and $\gamma = 0$, the state vector $|\Psi'\rangle$ in the basis of the M' sublevels (ordered from $M' = -2$ to $M' = +2$) of level $^3P_2$ reads as

$$|\Psi'\rangle = \frac{1}{\sqrt{2}}\begin{bmatrix} -\cos(\xi/2-\alpha) \\ i\sin(\xi/2-\alpha) \\ 0 \\ -i\sin(\xi/2-\alpha) \\ \cos(\xi/2-\alpha) \end{bmatrix}, \quad (4)$$

with the relative phase $\xi = 2(\chi + \phi)$. The filter laser optically pumps the populations out of states $M' = \pm 1$. The population remaining in states $M' = \pm 2$ depends on the phase ξ. In order to measure the population in states $M' = \pm 2$ the atoms travel through a magnetic field (inducing more than 100 Larmor cycles), which causes a uniform distribution of the population over the M' states since the velocity spread is $\Delta v/v \approx 0.35$ (FWHM). An unpolarized detection laser transfers the population of the $^3P_2$ level into the level $^3D_2$, from where fluorescence to the ground state is detected. The measured signal $S(\alpha)$ is proportional to the total population in states $M' = \pm 2$ [see Eq. (4)],

$$S(\alpha) = p\cos^2(\xi/2 - \alpha), \quad (5)$$

where p is the detection probability. For an incoherent superposition the modulation vanishes, as can be seen from Eq. (5) by averaging over the phase ξ.

It is also possible to determine the phase ξ by measuring the fluorescence induced by the filter laser. However, when this is done the emission characteristic needs to be taken into account, since the fraction of light detected depends on the direction of the laser polarization, which is rotated.

In the experiment, a beam of neon atoms emerges from a water cooled cold cathode discharge nozzle source. A fraction of the order of 10^{-4} of the atoms is in the metastable states $^3P_0$ or $^3P_2$ of the $2p^5 3s$ electronic configuration. The flow velocity of the atoms is about 800 ms^{-1} with a width of about 300 ms^{-1} (FWHM). The beam is collimated using a skimmer of 1 mm

diameter and a 50 μm slit positioned 183 cm apart. The population of the $^3P_2$ level of the ^{20}Ne isotope is depleted by optical pumping: A preparation laser ($\lambda = 633$ nm, not shown in Fig. 2) excites the atoms to the $^3D_2$ level of the $2p^5 3p$ configuration from where the atoms decay either back to the $^3P_2$ level or to the $^1S_0$ ground state via the short lived $^3P_1$ and $^1P_1$ states [see Fig. 1(b)]. Since the interaction time with the preparation laser is long compared to the lifetime of the excited level, all atoms are eventually removed from the metastable $^3P_2$ state.

The collimated neon beam enters the main chamber and intersects the pump, Stokes, and filter laser at right angles (see Fig. 2). The atoms in the $^3P_2$ level are detected 45 cm further downstream by a channeltron using laser induced fluorescence (LIF) on the $^3P_2 \leftrightarrow {}^3D_2$ transition, thus allowing state selective probing of the $^3P_2$ state. In the region between the STIRAP-zone and the filter laser magnetic fields are actively compensated by three pairs of external coils in Helmholtz arrangement to a residual field below 1 μT. The bandwidth of the servo loop is 1 kHz, which is adequate to compensate time varying homogeneous fields from nearby power supplies.

Three independent continuous single mode dye lasers are used in this experiment. All laser beams are delivered to the apparatus by single mode fibers. The state of polarization is controlled by fiber polarizers at the fiber exits followed by Glan-Taylor prisms, leading to a degree of polarization in the main chamber limited to 10^{-3} due to birefringence of the windows. Simulations show that this degree of polarization is adequate for the present purpose. The Stokes beam passes through a rotatable $\lambda/2$ wave plate which allows an arbitrary setting of the angle χ (see Fig. 2). Before entering the experimental chamber the filter beam passes a $\lambda/2$ wave plate controlled by a stepper motor. During data acquisition α is changed from 0 to 4π in 1600 steps. The data accumulation time is 50 ms per data point. In Fig. 3 a typical LIF signal $S(\alpha)$ is shown. The observation of a modulation is a direct proof of the coherence between the states $|2, -1\rangle$ and $|2, +1\rangle$. For a pure superposition the modulation depth would be 100%. The smaller degree of modulation is due to small magnetic fields (see below) and spontaneous emission during the detection process: During the action of the filter laser about 9% of the population pumped into the upper state $^3P_1$ decays back to the $^3P_2(M = \pm 2)$ state, leading to an incoherent background. The modulation depth of the signal agrees well with simulations including spontaneous emission and a small residual magnetic field, which causes a spread in the phase $\Delta\xi$ because of the velocity spread in the beam, thus leading to a signal averaged over $\Delta\xi$. The phase of the superposition is controlled by the angle χ of the Stokes polarization (see Fig. 2), which provides a simple and robust tool for manipulating the superposition. Figure 4 confirms a linear dependence, with a slope of unity, between the preset phase and the measured phase. Hence our technique allows one to write in and read out any given phase of the superposition (2).

Because the superposition involves Zeeman sublevels of the metastable $^3P_2$ state it is not subjected to spontaneous emission on a time scale <1 s. Decoherence occurs only via external magnetic fields or collisions within the beam.

We also measured the influence of a magnetic field $\mathbf{B}$ on the phase ξ. The $\mathbf{B}$ field leads to an additional term,

$$\hat{H}_B = g\frac{\mu_B}{\hbar}\mathbf{B}\hat{\mathbf{J}}, \tag{6}$$

in the Hamiltonian. Here g is the Landé factor, μ_B the Bohr magneton, and $\hat{\mathbf{J}}$ the angular momentum operator. For a magnetic field in the z direction ($\mathbf{B} \parallel \hat{e}_P$) the $|J, M\rangle$ states are eigenstates of the Hamiltonian (6); thus the superposition (2) acquires an additional phase,

$$\phi_B = g\frac{\mu_B}{\hbar}B_z T_{\text{flight}}, \tag{7}$$

varying linearly with B_z, as seen in Fig. 5 (top graph). Thus, a magnetic field may be used as an additional tool for controlling the phase of the superposition, although the velocity spread in the neon beam leads to a spread of T_{flight} and thus to a spread of the phase ϕ_B. For higher magnetic fields this spread washes out the modulation, as can be seen in Fig. 5 (bottom graph).

Obviously, good control over the magnetic fields for particles with a nonzero magnetic moment is needed in

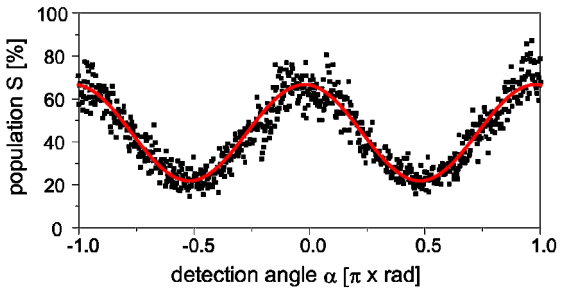

FIG. 3 (color online). Population $S(\alpha)$ as a function of the polarization angle α of the filter laser (see Fig. 2). The line is a $\cos^2$ fit to obtain the phase of the superposition.

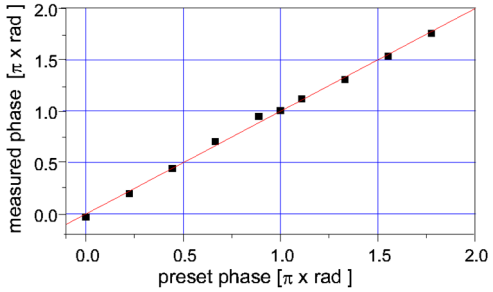

FIG. 4 (color online). Measured phase versus preset phase. The preset phase is controlled by the polarization angle χ of the Stokes laser. The line is a linear fit with a slope of unity.

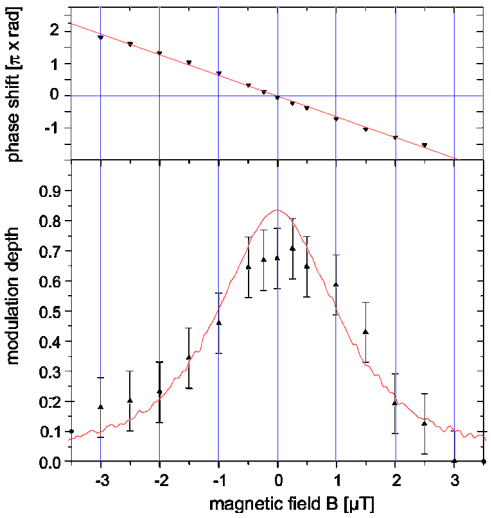

FIG. 5 (color online). Measured phase as a function of the magnetic field in the z direction (upper graph). The line is a linear fit. Dependence of the modulation depth on the magnetic field (bottom graph). The line origins from a Monte Carlo simulation including the velocity distribution of the beam.

the region between the creation and the measurement of the superposition, to establish a well-defined phase.

Magnetic fields perpendicular to the quantization axis lead to a redistribution of the population between the Zeeman sublevels due to Larmor precessions. This influence can be modeled but will not be discussed here.

In conclusion, we have demonstrated experimentally a technique for preparing a well-defined superposition of two magnetic sublevels based upon tripod-STIRAP. The use of a linearly polarized Stokes field guarantees that the two states in the created superposition have equal amplitudes. The relative phase of the superposition can be controlled by the polarization angle χ of the Stokes field. Because the population transfer vehicle is a dark state, this technique is immune to loss of coherence and population due to spontaneous emission from the intermediate state $^3P_1$. We have also demonstrated a method for accurate measurement of the phase of the created superposition, based on mapping the superposition parameters onto the populations of the magnetic sublevels and observing the population in a subset of these states.

The accuracy of both the creation and the measurement techniques, and the elimination of decoherence, suggests a significant potential for the use of these techniques in quantum information algorithms, where high fidelity is crucial. Potential applications to quantum information include the use of tripod-STIRAP as an initialization technique that prepares a well-defined arbitrary superposition of $|J, M\rangle$ states. Tripod-STIRAP can also be used to create and manipulate coherent superpositions of three states, e.g., $|0, 0\rangle$, $|2, -1\rangle$, and $|2, +1\rangle$, which can be used as a qutrit. The measurement technique is not limited to the specific tripod-STIRAP technique but can be used in general to read the parameters of a qubit created and manipulated by some other technique.

We thank S. Mossmann and R. Unanyan for the discussions. This work has been supported by the European Union Research Training network COCOMO, Contract No. HPRN-CT-1999-00129 and Marie-Curie-training-site Contract No. HPMT-CT-2001-00294 as well as by the Deutsche Forschungsgemeinschaft. N. V. V. acknowledges support by the Alexander von Humboldt Foundation.

*Electronic address: vewinger@physik.uni-kl.de
†Permanent address: Department of Physics, Sofia University, James Boucher 5 blvd., 1126 Sofia, Bulgaria.
‡http://www.physik.uni-kl.de/bergmann/

[1] R. Unanyan, M. Fleischhauer, B.W. Shore, and K. Bergmann, Opt. Commun. **155**, 144 (1998).
[2] H. Theuer, R. G. Unanyan, C. Habscheid, K. Klein, and K. Bergmann, Opt. Express **4**, 77 (1999).
[3] U. Gaubatz, P. Rudecki, S. Schiemann, and K. Bergmann, J. Chem. Phys. **92**, 5363 (1990); K. Bergmann, H. Theuer, and B.W. Shore, Rev. Mod. Phys. **70**, 1003 (1998).
[4] D. Bouwmeester, A. Ekert, and A. Zeilinger, *The Physics of Quantum Information: Quantum Cryptography, Quantum Teleportation, Quantum Computation* (Springer-Verlag, Berlin, 2000).
[5] F. Schmid-Kaler, H. Häffner, M. Riebe, S. Gulde, G. P. T. Lancaster, T. Deuschle, C. Becher, C. F. Roos, J. Eschner, and R. Blatt, Nature (London) **422**, 408 (2003); D. Leibfried, B. DeMarco, V. Meyer, D. Lucas, M. Barrett, J. Britton, W. M. Itano, B. Jelenković, C. Langer, T. Rosenband, and D. J. Wineland, Nature (London) **422**, 412 (2003).
[6] N. A. Gershenfeld and I. L. Chuang, Science **275**, 350 (1997).
[7] G. Burkard, D. Loss, and D. P. DiVincenzo, Phys. Rev. B **59**, 2070 (1999).
[8] Y. Makhlin, G. Schön, and A. Shnirman, Nature (London) **398**, 305 (1999).
[9] F. Yamaguchi and Y. Yamamoto, Appl. Phys. A **68**, 1 (1999).
[10] A. S. Parkins, P. Marte, P. Zoller, and H. J. Kimble, Phys. Rev. Lett. **71**, 3095 (1993).
[11] P. Domokos, J. M. Raimond, M. Brune, and S. Haroche, Phys. Rev. A **52**, 3554 (1995).
[12] C. S. Adams, M. Sigel, and J. Mlynek, Phys. Rep. **240**, 143 (1994).
[13] J. Marangos, J. Mod. Opt. **45**, 471 (1998).
[14] A. Nottelmann, C. Peters, and W. Lange, Phys. Rev. Lett. **70**, 1783 (1993).
[15] P. Brumer and M. Shapiro, Annu. Rev. Phys. Chem. **43**, 257 (1992).
[16] J. B. Watson, A. Sanpera, X. Chen, and K. Burnett, Phys. Rev. A **53**, R1962 (1996).
[17] R. N. Zare, *Angular Momentum - Understanding Spatial Aspects in Chemistry and Physics* (John Wiley & Sons, New York, 1988).